JOURNAL OF GEOPHYSICAL RESEARCH, VOL. 102, NO. D15, PAGES 18,879–18,888, AUGUST 20, 1997

Emissions of organic trace gases from savanna fires in southern Africa during the 1992 Southern African Fire Atmosphere Research Initiative and their impact on the formation of tropospheric ozone

R. Koppmann, A. Khedim, J. Rudolph, and D. Poppe
Institut für Atmosphärische Chemie, Forschungszentrum Jülich, Jülich, Germany

M. O. Andreae, G. Helas, M. Welling, and T. Zenker
Max-Planck-Institut für Chemie, Mainz, Germany

Abstract. CO, CH_4, and organic trace gases were measured in air samples collected during several flights with a DC-3 aircraft through the plumes from savanna fires and agricultural fires during the SAFARI 92 campaign in southern Africa in September and October 1992. In all samples a variety of higher molecular weight organic compounds was found, most of which are very reactive. More than 70 of the roughly 140 major components present could be identified. Typically, mixing ratios of several hundred parts per billion carbon of organic compounds were measured inside the plumes, corresponding to an emission ratio of total organic carbon relative to CO_2 of up to 1%. About 50% of these emissions were in the form of oxygenated and unsaturated compounds. The contributions of still unknown compounds to the total emission of organic compounds add up to another 20–30%. The observed emission ratios relative to CO_2 show a considerable variation depending on the fuel type and the burning stages of the fire. The lowest value of the emission ratio of the sum of all identified organic compounds relative to CO_2 was found for a sugar cane fire with $(1.7 \pm 0.7) \times 10^{-3}$ (ppb C/ppb CO_2). For a large savanna fire in Kruger National Park the ratio was $(7.4 \pm 1.6) \times 10^{-3}$ (ppb C/ppb CO_2). The highest value was $(13.7 \pm 0.9) \times 10^{-3}$ (ppb C/ppb CO_2) for an uncontrolled fire of mainly wood and shrub in the Drakensberg region. Results of model calculations show that in biomass-burning plumes, reactive organic compounds contribute significantly to the formation of ozone, especially during the initial phase of photochemical processing.

Introduction

Emissions from biomass burning are known to be a considerable source of atmospheric hydrocarbons, especially in tropical and subtropical regions [*Greenberg et al.*, 1984; *Greenberg and Zimmerman*, 1984; *Crutzen et al.*, 1985; *Zimmerman et al.*, 1988; *Rasmussen and Khalil*, 1988; *Bonsang et al.*, 1991; *Rudolph et al.*, 1992, 1995]. Owing to transport, these emissions have also a significant impact on the budget of organic trace gases in the tropical marine atmosphere [*Koppmann et al.*, 1992; *Swap et al.*, 1996]. Moreover, owing to their impact on photochemical ozone formation, organic trace gases influence the budget of tropospheric ozone [*Chatfield and Delany*, 1990; *Fishman et al.*, 1990; *Helas et al.*, 1995; *Thompson et al.*, 1996]. The biomass burned annually on a global scale is estimated to be about 8.6×10^{15} g of dry material, 45% of which is savanna grassland [*Levine*, 1991]. Savanna fires are thus the largest single source of biomass-burning emissions.

In recent years a growing number of studies were published that deal with field measurements of emissions from biomass burning in Africa, which contains about two thirds of the world's savanna regions [*Delmas*, 1982; *Bonsang et al.*, 1991; *Rudolph et al.*, 1995; *Lacaux et al.*, 1995]. These data were obtained from both ground-based and airborne measurements in the vicinity of and over large fires. The results showed that during the biomass-burning season the concentrations of CO and organic trace gases in the planetary boundary layer were considerably enhanced over those in the wet season [*Rudolph et al.*, 1992]. Meanwhile, laboratory experiments have supplied more information about the parameters that determine the emission factors, such as different burning stages, meteorological conditions, and fuel types [*Lobert et al.*, 1991; *Manø*, 1997; *Czapiewski*, 1995]. It has been shown that the burning of organic material in oxygen-deficient fires leads to the emission of methane, nonmethane hydrocarbons (NMHC), and a variety of partially oxidized organic compounds. In some cases the emissions of medium- and higher-molecular-weight organic compounds exceed those of light NMHC. Thus these emissions contribute significantly to the local budgets of organic trace gases in the regions of biomass burning and may have a considerable impact on the formation of ozone in these areas. Very recent studies showed the significant abundance of higher-molecular-weight volatile organic compounds (VOC) in biomass-burning plumes. However, only the sum over all organic compounds on a parts per billion (ppb) carbon basis were given without specifying the contributions of individual compounds [*Hurst et al.*, 1994]. The aim of the present paper is to study the variety of VOC that are emitted by biomass burning. The data

Paper number 97JD00845.
0148-0227/97/97JD-00845$09.00

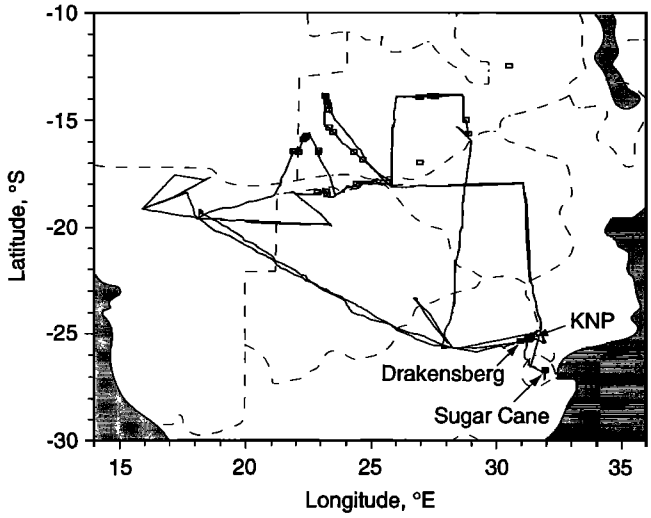

Figure 1. Flight tracks of the SAFARI project. The sampling locations for this study are indicated.

were obtained during the airborne measurements of the Southern African Fire-Atmosphere Research Initiative (SAFARI) campaign in southern Africa, which was conducted under the International Geosphere-Biosphere Program (IGBP) core project International Global Atmospheric Chemistry (IGAC). The objectives and a summary of the main results are given by *Andreae et al.* [1994] and *Fishman et al.* [1996]. Flask samples were collected from different types of fire in order to investigate the composition of biomass-burning emissions. Parts of these measurements are used to estimate the impact of VOC on the photochemical ozone formation. Special emphasis is placed on VOC with five or more carbon atoms since ozone formation in biomass-burning plumes during the initial phase of the photochemical processing cannot be explained with the oxidation of CH_4, CO, and light NMHC alone. Although the existing data on the organic composition of biomass-burning plumes are limited, it can be expected that many of the higher-molecular-weight VOC are very reactive and thus contribute significantly to the photochemistry in the plumes.

Experiment

During SAFARI 92, prescribed savanna fires in the Kruger National Park (South Africa) and sugar cane fires as well as uncontrolled fires were investigated. Before the prescribed fires were ignited, the fuel load, fuel type, and spatial distribution were measured within the burning areas [*Stocks et al.*, 1996]. During the fires a large set of trace compounds and aerosols were measured from ground-based and airborne platforms [*Andreae et al.*, 1996; *Le Canut et al.*, 1996]. The fire stages and burning conditions were controlled and monitored during the campaign. After the fires, the type and amount of the remaining biomass as well as the ash were analyzed.

The measurements discussed here are based on samples collected on three flight legs. During flight SAF04 on September 19, 1992, the plumes of two prescribed sugar cane fires on the Ubombo Ranches plantation near Big Bend, Swaziland, were probed. It is standard regional agricultural practice to set such fires before harvesting to facilitate the cutting and processing of the sugar cane. The two fields had an area of 12 and 43.7 ha, respectively. A controlled burn on block 55 (2333 ha) in the Pretoriuskop section of the Kruger National Park was investigated during flight SAF06 on September 24, 1992. Details on fuel and fire behavior are given by *Stocks et al.* [1996], and details on particle emissions are given by *Le Canut et al.* [1996]. During flight SAF05 on September 20, 1992, an uncontrolled "fire of opportunity" in the Drakensberg region was encountered. The burned biomass was a mixture of forest, shrub, and grass.

Sampling was done aboard a DC-3 aircraft operating between 100 m and 4000 m altitude. Figure 1 gives an overview of the flight tracks of the SAFARI project and the sampling locations for this study.

Sampling

About 120 whole air samples were collected in evacuated stainless steel canisters of 2-L volume. Figure 2 shows a schematic drawing of the air-sampling system. The air intake was a stainless steel tube (6-mm ID) mounted on the top the aircraft extending beyond the boundary layer of the DC-3. The exhaust line was mounted in the back of the aircraft. Once the DC-3 was airborne, the inlet line was continuously flushed with ambient air. The air samples were pressurized with a metal bellows pump to a pressure of about 300 kPa. Typical sampling times were between 1 and 2 min depending on the altitude of the aircraft. This time is comparable to the transit time through the plumes. The dates, times, locations, and altitudes of the plume samples are given in Table 1.

Analysis

The samples were analyzed in the laboratory in Jülich, Germany, by gas chromatography for CO, CO_2, CH_4, and nonmethane hydrocarbons. CO, CO_2, and CH_4 were determined by a gas chromatographic method very similar to the one described by *Heidt* [1978]. The precision is 3% for CO, 0.5% for CO_2 and 1% for CH_4. The higher-molecular-weight VOC were analyzed using gas chromatography with flame ionization (FID) and electron capture (ECD) detectors. The hydrocarbons were preconcentrated cryogenically from volumes between several hundred milliliters and about 2 L depending on the expected concentrations in the plume samples and background samples and separated on a combination of a 7-m micropacked Porapack QS column and a 105-m RTX-1 fused silica capillary column. The detection limits were between 10 ppt (parts per trillion) for the measurements on the packed column (C_2–C_4 hydrocarbons) and below 1 ppt for the mea-

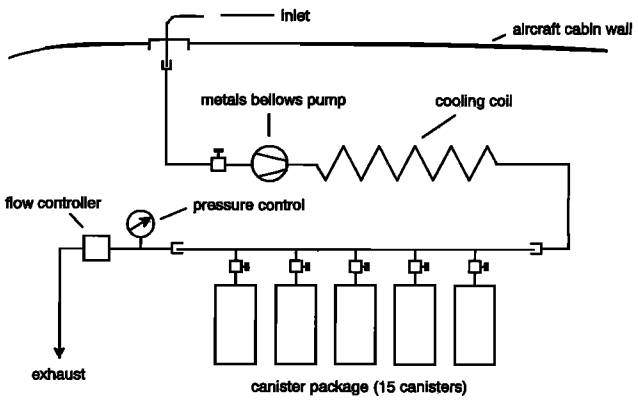

Figure 2. Schematic drawing of the sampling system installed on board the DC-3.

Table 1a. Plume Samples From the Sugar Cane Fire During Flight SAF04 on September 19, 1992

Sample	Sampling Time, UT	Latitude, °S	Longitude, °E	Altitude, m	Passage	CH_4, ppb	CO, ppb	CO_2, ppm
			Sugar Cane Field 1 Plume					
3583	0703	26.73	32.00	489	1	1938	2586	392
3584	0706	26.74	32.01		2	1874	2444	396
3585	0711	26.71	32.00	327	4	1866	4469	549
3586	0714	26.72	32.00	313	5	1832	4403	534
			Sugar Cane Field 2 Plume					
3588	0745	26.72	31.94	778	10	1797	2814	463
3589	0748	26.71	31.94	363	11	1837	5407	644
3590	0810	26.78	31.94	291	18	2036	2980	485
Mean						1883	3587	495
s.d.						80	1157	89

Plume crossings are identified by broad maxima in the continuous CO and CO_2 measurements. The time for one plume passage was between 1 and 2 min, and the sampling time was about 1 min.

surements on the capillary column (C_5–C_{10} organic trace gases). The reproducibility ranged between 10 and 30% depending on the compound. Details of the analytical techniques are given by *Koppmann et al.* [1992, 1993] and *Rudolph et al.* [1986, 1995].

For a number of plume samples the medium-molecular-weight organic trace gases (C_5–C_{10}) were additionally analyzed with a mass spectrometer (Fisons, MD 800). For this purpose the effluent of the capillary column was split with a ratio of 3:1 between the FID detector and the mass spectrometer (MS). The FID was used for quantification of the compounds in the sample, and the MS was used for identification purposes. With this technique is was possible to record mass spectra even of compounds with mixing ratios as low as a few parts per trillion. It should be noted that this technique, including the sampling in stainless steel canisters, is not an adequate method for all organic compounds that can be observed in the samples. It is well known that reactive and highly polar compounds are not stable in canisters or in stainless steel lines and that others cannot be preconcentrated and desorbed quantitatively [*Rudolph et al.*, 1990]. For these types of compounds the mixing ratios and emission ratios given here should therefore be considered as lower limits. Significant losses in the canisters and in our preconcentration system due to reactions with ozone can be excluded owing to the fast decay of ozone on stainless steel surfaces [*Greenberg et al.*, 1992; *Koppmann et al.*, 1995].

Results and Discussion

Organic Composition of Biomass-Burning Emissions

Vegetation material is made up of cellulose, hemicelluloses, lignin, proteins, nucleic acids, amino acids, and volatile substances [*Franke*, 1989]. During the first phase of a fire the volatile compounds such as aldehydes, alcohols, and terpenes are released. In the following phase, thermal cracking of the fuel molecules occurs. Higher-molecular-weight compounds are decomposed into a variety of volatile organic compounds [*Lobert and Warnatz*, 1993]. In addition to the light hydrocarbons, which were the only organic compounds investigated in previous field studies, a large number of higher-molecular-weight organic trace gases is expected in the emissions from biomass burning. They include alcohols, aldehydes, ketones, carboxylic acids, esters, ethers, furanes, etc. These partly oxidized compounds are predominantly emitted during the smoldering phase of fires [*Czapiewski*, 1995]. Figure 3 shows a capillary column chromatogram of $\geq C_5$ VOC of an air sample collected inside the plume of the Drakensberg fire during flight SAF05 (sample 3602). The mixing ratios of CO_2 and CO in this sample were 399.5 ppm and 4420 ppb, respectively. The average $\Delta(CO)/\Delta(CO_2)$ ratio (calculated from samples collected during all passages through the plume) was 9.36 ± 1.30%. This indicates a mix of flaming and smoldering combustion at the

Table 1b. Plume Samples From the Drakensberg Fire During Flight SAF05 on September 20, 1992

Sample	Sampling Time, UT	Latitude, °S	Longitude, °E	Altitude, m	Passage	CH_4, ppb	CO, ppb	CO_2, ppm
3593	1106	25.30	31.09	1039	1	2022	2907	384
3592	1110	25.28	31.07	1160	2	1831	1100	368
3594	1114	25.29	31.09	1110	3	2039	3100	383
3595	1117	25.28	31.11	1069	4	1986	2764	382
3596	1120	25.28	31.10	1013	5	1902	1719	374
3598	1130	25.47	30.69	1656	6	1825	975	369
3599	1133	25.45	30.72	1701	7	1833	1150	372
3601	1142	25.44	30.70	1303	8	2103	3413	389
3602	1145	25.45	30.70	1463	9	2236	4417	400
Mean						1976	2394	380
s.d.						141	1210	10

Nine passages through this plume were flown during flight SAF05. Plume crossings are identified by broad maxima in the continuous CO and CO_2 measurements. The time for one plume passage was about 2 min, and the sampling time was about 1 min.

Table 1c. Plume Samples from the Kruger National Park Fire 2 (Block 55) During Flight SAF06 on September 24, 1992

Sample	Sampling Time, UT	Latitude, °S	Longitude, °E	Altitude, m	Passage	CH_4, ppb	CO, ppb	CO_2, ppm
3610	1041	25.27	31.32	1423	3	1868	2243	398
3611	1043	25.20	31.32	1359	4	1883	3007	410
3613	1047	25.29	31.35	1442	5	1791	1061	374
3614	1053	25.25	31.33		7	1861	2226	393
3616	1057	25.29	31.29	1756	8	1747	442	365
3617	1059	25.21	31.32	1760	9*	1833	1860	398
3618	1101	25.26	31.32	1730	9*	1779	899	370
3620	1105	25.28	31.31	1754	10	1812	1508	384
Mean						1822	1656	386
s.d.						48	842	16

Eight samples were taken during a total of 22 passages through this plume during flight SAF06. Plume crossings are identified by broad maxima in the continuous CO and CO_2 measurements. Typical times for one plume passage were between 1.5 and 2 min; the sampling time in all cases was about 1 min.

*Two samples were taken in the same plume. The time for passage 9 was 3.5 min.

time of the plume passages. The sum over the mixing ratios of C_2 and C_3 hydrocarbons was 364 ppb C. For the analysis of this sample the mass spectrometer was used in parallel to the FID and ECD. More than 140 major peaks are found in this chromatogram, about 70 of which could be identified. Table 2 gives the retention times of the peaks and the identification of the compounds. In a first step these compounds were identified by comparing the mass spectra with MS data from the U.S. National Institute of Standards and Technology (NIST) library. In some cases two or more compounds overlapped into one peak. These compounds are included only if an identification of at least one compound (agreement better than 90%) was possible. This was then verified by comparing the relative retention times and the known boiling point of the compounds. The quantitative analysis of the organic compounds was based on the FID response. The response of the FID is proportional to the molar mass of the compounds; i.e., within one group of organic trace gases the response increases linearly with the mass of the molecule. The response, however, is slightly different for groups of compounds with hetero atoms such as oxygen, nitrogen, and sulfur or for compounds with different functional groups. Generally, in these cases the response is lower than for "pure" hydrocarbons. Because for this analysis we treated all compounds as "pure" hydrocarbons and because of the aforementioned problems of a quantitative determination of some of these compounds, our emission ratios can be seen as lower limits; i.e., the "real" emission ratios may be higher than the values given here.

As a result of this analysis a large number of organic trace gases could be identified that were previously not known to be emitted by biomass burning. In general, the mixing ratios of the different members of the various compound groups decrease with increasing number of carbon atoms. This is in good agreement with laboratory studies carried out with tropical wood which showed very similar emission patterns [*Czapiewski*, 1995]. From these data, emission ratios are calculated on a ppb carbon basis, and the contribution of these compounds to the total emission of organic trace gases and relative to CO and CO_2 can be derived.

Emission Ratios of Organic Trace Gases

CO_2 is the dominant carbon species emitted from fires, followed by CO. The emission ratio of CO relative to CO_2, $\Delta CO/\Delta CO_2$, is used to characterize the different burning stages. During the flaming phase this ratio is relatively low, in general, 5–10%. During the smoldering phase of a fire, more CO is

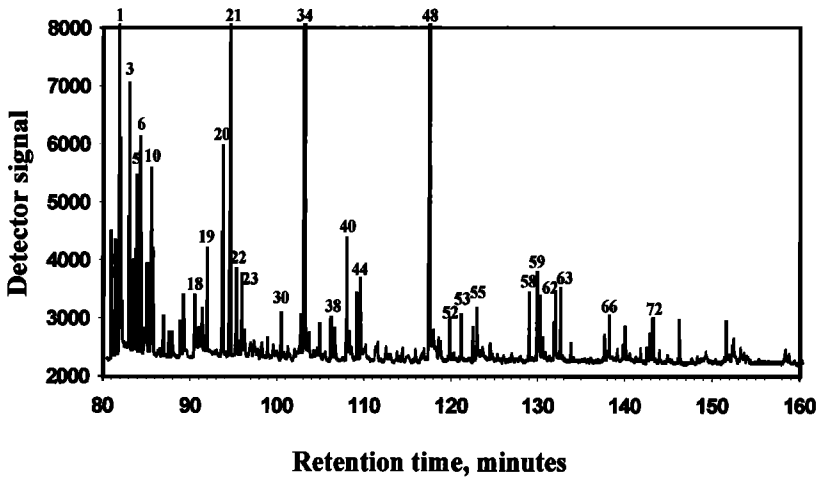

Figure 3. Chromatogram of sample 3602. The major peaks are identified by numbers. The numbers in the chromatogram correspond to the numbers given in Table 2.

emitted owing to low oxygen supply, and the ratio of $\Delta CO/\Delta CO_2$ increases. Typical values observed during this phase vary between 10 and 15%. Also, the emissions of organic compounds vary as a function of the burning stages. The correlation of an organic trace gas with CO_2 the emission ratios of that trace gas to be estimated as a function of type of fire and the different burning processes and the burning stages.

Table 3 summarizes the emission ratios of the two sugar cane fires, the Kruger National Park fire, and the Drakensberg fire for CO, CH_4, the sum of C_2–C_4 hydrocarbons, and the sum of organic trace gases with five or more carbon atoms. The total amount of organic trace gases with five or more carbon atoms is based on all FID-responsive compounds found in the chromatograms. Table 4 gives the individual emission ratios for the most abundant organic compounds identified. In all cases the highest emission ratios were observed for the Drakensberg fire, while the sugar cane fires showed the lowest emission ratios. As was mentioned above, the emission ratio of CO relative to CO_2 allows the burning conditions of the different fires to be characterized. For the fire at Drakensberg, smoldering is likely to be the dominant burning process, while the sugar cane fires were largely flaming fires. The fire of block 55 in the Kruger National Park seemed to be a mixture of both. The flaming phase of the fire was followed by a brief smoldering phase. Since this fire covered a large savanna area, emissions from both phases of the fire converge in the smoke plumes, leading to the observed emission ratios. It can be seen that the emissions of the sum of the light NMHC are comparable or even larger than the emission ratio of methane. This has already been observed during previous field studies of large savanna fires with similar $\Delta CO/\Delta CO_2$ ratios in Africa and Australia [*Bonsang et al.*, 1991; *Rudolph et al.*, 1992; *Hurst et al.*, 1994]. Our results show further that the emission ratio of organic compounds with carbon number of 5 or more add up to at least half of the contribution of light NMHC.

The emission ratios of the total measured organic compounds relative to CO_2 were $(13.7 \pm 0.9) \times 10^{-3}$ (ppb C/ppb CO_2) for the Drakensberg fire, $(7.4 \pm 1.6) \times 10^{-3}$ (ppb C/ppb CO_2) for the Kruger National Park fire, and $(3.9 \pm 2.9) \times 10^{-3}$ and $(1.7 \pm 0.7) \times 10^{-3}$ (ppb C/ppb CO_2) for sugar cane fires 1 and 2, respectively. These values compare well with measurements of fires under laboratory conditions as reported by *Manø* [1997] and *Czapiewski* [1995], who give an average emission ratio of the sum of organic compounds for their experiments of 8.4×10^{-3} and 3×10^{-3}, respectively. *Lobert et al.* [1991] report an average of 11.9×10^{-3} based on 10 different experiments. The ratio found for the Kruger National Park fire is in good agreement with the laboratory measurements, while the ratio found for the Drakensberg fire exceeds the laboratory values. The emission ratios of the predominantly flaming sugar cane fires are considerably lower than the results of the laboratory studies. This may be due to the fact that large flaming combustion can not be simulated realistically in confined fires, which are controlled by their artificial boundaries. Especially the response of fires to wind and the access to oxygen for combustion, which affects mainly the flaming phases, differs significantly between free and confined fires [*Albini*, 1993].

Impact of Volatile Organic Compounds

Ozone Formation

In order to estimate the impact of VOC on the formation of ozone in biomass-burning plumes we conducted a simple

Table 2. Compounds Positively Identified in Sample 3602

Peak	Retention Time, min	Identification
1	81.61	acetone
2	81.81	*i*-pentane
3	82.82	1-pentene
4	83.30	2-methyl-1-butene
5	83.66	n-pentane
6	84.08	isoprene
7	84.21	(E) 2-pentene
8	84.60	2-methyl-2-propanol
9	84.89	methylacetate
10	85.34	2-methyl-2-butene
11	85.57	(E) 1,3-pentadiene
12	85.91	1,2-pentadiene
13	86.36	CS_2 + ?
14	86.74	(Z) 1,3-pentadiene
15	87.77	propanenitrile
16	88.68	tetrahydrofuran
17	89.08	cyclopentane
18	90.33	methylvinylketone + 2-methyl-1-pentane
19	91.75	butanal
20	93.60	1-hexene
21	94.42	2-methylfuran
22	95.04	ethylacetate
23	95.21	*n*-hexane
24	95.81	3-methylfurane
25	96.15	4-methyl-2-pentene
26	97.26	2-methyl-1-propanol + ??
27	98.13	4-methyl-2-pentene
28	98.77	2,3-dihydrofuran
29	99.47	methylcyclopentane
30	100.37	3-methylbutanal
31	101.15	3-methylbutanon
32	101.91	1-butanol
33	102.59	2,4-hexadiene
34	102.95	benzene
35	103.59	thiophene
36	104.51	1-penten-3-one
37	104.82	2-pentanone
38	106.09	cyclopentanal
39	106.57	cyclohexane
40	107.94	1,2-dimethylcyclopentane
41	108.27	trichlorethene
42	108.50	2-ethylfuran
43	109.07	2,4-dimethylfuran + 3-hexen-1-ol-acetate
44	109.51	*n*-heptane
45	111.26	phenol
46	112.47	2-hexanone + ??
47	113.74	dimethylsulfide
48	117.41	toluene
49	117.96	2-methylheptane
50	118.20	2.2-dimethylpentanal
51	118.56	dimethylcyclohexane
52	119.82	hexanal
53	121.05	1-octene
54	122.45	acetic acid 2-methylpropylester
55	122.91	n-octane
56	123.38	2-octene
57	123.62	2-furaldehyde
58	128.98	ethylbenzene
59	129.89	*p*,*m*-xylene + 3-heptanone
60	130.55	2-heptanone
61	131.81	styrene
62	132.00	7-methyl-1-octene
63	132.61	*o*-xylene
64	133.81	*n*-nonane
65	137.68	6-methyl-2-heptanone
66	138.24	benzaldehyde
67	139.18	propylbenzene
68	139.84	1-ethyl-3-methylbenzene
69	140.01	benzonitrile + ??
70	140.62	1,2,4-trimethylbenzene
71	141.85	1-ethyl-4-methylbenzene
72	143.28	benzofuran

Table 3. Emission Ratios of Methane, Carbon Monoxide, Light NMHC and Higher-Molecular-Weight Organic Trace Compounds Calculated From the Plume Samples

Passage	$\Delta(CO)/\Delta(CO_2)$, %	$\Delta(CH_4)/\Delta(CO_2)$, %	$\Delta(\Sigma\ C_2\text{–}C_4)/\Delta(CO_2)$, %	$\Delta(\Sigma\ C_5\text{–}C_9)/\Delta(CO_2)$, %
		Flight SAF04, Sugar Cane Field 1		
1	6.97	0.57	0.22	0.16
2	5.90	0.35	0.59	0.27
4	2.25	0.07	0.13	0.06
5	2.41	0.05	0.10	0.04
Mean	4.38	0.26	0.26	0.13
s.d.	2.09	0.22	0.20	0.09
		Flight SAF04, Sugar Cane Field 2		
10	2.52	0.05	0.11	0.05
11	1.83	0.03	0.07	0.02
18	2.21	0.23	0.18	0.08
Mean	2.19	0.11	0.12	0.05
s.d.	0.28	0.09	0.05	0.02
		Flight SAF05, Drakensberg		
1	9.81	1.04	0.40	0.41
2	8.77	0.93	1.92	0.54
3	11.53	1.27	0.99	0.48
4	10.46	1.05	0.87	0.43
5	9.22	1.07	0.77	0.40
6	7.32	0.78	0.68	0.37
7	7.36	0.72	0.72	0.38
8	9.86	1.17	1.00	0.49
9	9.86	1.20	1.02	0.48
Mean	9.36	1.03	0.93	0.44
s.d.	1.30	0.17	0.40	0.05
		Flight SAF06, Kruger National Park Fire 2		
3	5.23	0.32	0.48	0.21
4	5.51	0.28	0.45	0.21
5	5.68	0.32	0.51	0.48
7	5.86	0.35	0.50	0.20
8	4.15	0.10	0.38	0.38
9	4.27	0.23	0.35	0.16
9	6.37	0.34	0.54	0.35
10	5.26	0.28	0.44	0.23
Mean	5.29	0.28	0.46	0.28
s.d.	0.71	0.07	0.06	0.10

model calculation using the regional acid deposition model (RADM2) published by *Stockwell et al.* [1990]. We are aware of the fact that RADM2 was not originally designed for a VOC mix as observed in biomass-burning plumes, and not all measured organic compounds are accounted for individually. They are lumped according to their reactivity with regard to OH radicals. The substantial contributions from the light hydrocarbons are taken explicitly into account. Nevertheless, we used this model as a simplified approximation to simulate the formation of ozone in the plumes and get information about the contribution of VOC to this process.

The calculations were initialized with measured mixing ratios from the sugar cane fires, which showed the lowest VOC emission ratios, and the Drakensberg fire, which had the highest observed VOC emission ratios. The NO_2 mixing ratio was derived from the NO_2/CO_2 ratio given by *Andreae et al.* [1996] and our CO_2 measurements. The initial mixing ratios for short-lived trace gases that were not measured (OH, HO_2, NO, etc.) were derived from a steady state approximation. The solar zenith angle was fixed to 24°.

Under realistic conditions, ozone formation is substantially influenced by transport processes causing a dilution of the trace gases within the plume [e.g., *Lelieveld et al.*, 1997]. In order to account for this, we included dilution with surrounding air in our simulation. Initially, the plume is enclosed in a volume $V(0)$ that increases with time to the volume $V(t)$ thereby mixing in background air with fixed mixing ratios of $[CO]^0$ = 100 ppb, $[CH_4]^0$ = 1.7 ppm, $[O_3]^0$ = 50 ppb, and $[VOC]^0$ = 5 ppb C. The time dependence of $V(t)$ was parameterized by

$$V(t) = V(t_e) + (1 - V(t_e)) \exp(-t/\tau)$$

where τ is the time constant for dilution and $V(t_e)$ is the final size of the plume at the end of the integration at time t_e, assuming ($\tau \ll t_e$). The dilution factor is given by $D = V(t_e)/V(0)$. Measurements of air samples collected outside the plumes gave CO_2 mixing ratios that were on average 10 ppm above the global background. The dilution was treated in a way that the CO_2 mixing ratios measured in the plumes was finally reduced to the CO_2 mixing ratio observed in the air outside of the plumes.

In the case of the Drakenberg fire the final dilution was D = 2, and the dilution time constant was assumed to be τ = 2 hours. Ozone mixing ratios (initialized with a background value of 50 ppb) in the plume are shown in Figure 4. If only CH_4 and CO as oxidizable carbon compounds are taken into account, ozone reaches a maximum mixing ratio of 134 ppb after 30 sunlit hours. The VOC were included in two steps, first

Table 4. Mean and Standard Deviation of Emission Ratios of the Most Abundant Organic Trace Gases of Intermediate Molecular Weight Relative to Excess CO_2 (in ppb carbon) for the Different Types of Fires

Compound	Emission Ratio, ppb C		
	Drakensberg Fire	KNP Fire 2	Sugar Cane Fires
1-pentene	$(1.1 \pm 0.3) \times 10^{-4}$	$(5.8 \pm 1.3) \times 10^{-5}$	$(1.7 \pm 2.5) \times 10^{-5}$
2-methyl-1-butene	$(5.9 \pm 1.9) \times 10^{-5}$	$(0.5 \pm 1.0) \times 10^{-5}$	$(0.7 \pm 1.2) \times 10^{-5}$
2-methyl-2-butene	$(8.7 \pm 2.0) \times 10^{-5}$	$(1.8 \pm 1.2) \times 10^{-5}$	$(5.7 \pm 9.2) \times 10^{-6}$
4-methyl-1-pentene	$(7.9 \pm 3.5) \times 10^{-5}$	$(7.8 \pm 5.2) \times 10^{-5}$	$(2.7 \pm 3.5) \times 10^{-5}$
1-hexene	$(1.3 \pm 0.3) \times 10^{-4}$	$(8.4 \pm 1.1) \times 10^{-5}$	$(2.6 \pm 4.0) \times 10^{-5}$
1-octene	$(2.2 \pm 0.8) \times 10^{-5}$	$(1.6 \pm 0.8) \times 10^{-5}$	$(0.7 \pm 1.2) \times 10^{-5}$
2-octene	$(2.0 \pm 1.8) \times 10^{-6}$	—	$(2.8 \pm 3.1) \times 10^{-7}$
2-methyl-2-propanol	$(6.7 \pm 6.9) \times 10^{-6}$	$(6.1 \pm 7.0) \times 10^{-6}$	$(1.4 \pm 1.0) \times 10^{-5}$
1-butanol	$(6.0 \pm 1.8) \times 10^{-6}$	$(5.9 \pm 4.6) \times 10^{-6}$	$(3.8 \pm 5.7) \times 10^{-6}$
Cyclopentanol	$(5.0 \pm 2.5) \times 10^{-5}$	$(5.1 \pm 3.8) \times 10^{-5}$	$(2.8 \pm 3.0) \times 10^{-5}$
2-methyl-propanal	$(1.8 \pm 0.8) \times 10^{-5}$	$(1.3 \pm 0.9) \times 10^{-5}$	$(3.1 \pm 2.3) \times 10^{-6}$
Butanal	$(8.4 \pm 1.9) \times 10^{-5}$	$(6.7 \pm 6.1) \times 10^{-5}$	$(2.9 \pm 3.5) \times 10^{-5}$
3-Methylbutanal	$(2.4 \pm 0.7) \times 10^{-5}$	$(1.6 \pm 1.5) \times 10^{-5}$	$(7.4 \pm 9.3) \times 10^{-6}$
2,2-Dimethylpetanal	$(5.7 \pm 4.5) \times 10^{-6}$	$(1.2 \pm 2.5) \times 10^{-6}$	$(1.4 \pm 2.1) \times 10^{-6}$
Hexanal	$(4.9 \pm 2.8) \times 10^{-5}$	$(3.9 \pm 2.2) \times 10^{-5}$	$(1.9 \pm 1.3) \times 10^{-5}$
Benzaldehyde	$(4.2 \pm 1.9) \times 10^{-5}$	$(4.5 \pm 3.0) \times 10^{-5}$	$(1.4 \pm 1.3) \times 10^{-5}$
Acetic acid-2-methylpropylester	$(1.5 \pm 0.5) \times 10^{-5}$	$(8.2 \pm 0.5) \times 10^{-5}$	$(1.7 \pm 2.4) \times 10^{-6}$
3-methylbutanone	$(8.2 \pm 1.2) \times 10^{-6}$	$(7.5 \pm 5.2) \times 10^{-6}$	$(2.5 \pm 3.1) \times 10^{-6}$
1-penten-3-one	$(6.6 \pm 2.7) \times 10^{-6}$	$(4.4 \pm 2.5) \times 10^{-6}$	$(2.1 \pm 3.0) \times 10^{-6}$
2-pentanone	$(3.7 \pm 1.8) \times 10^{-5}$	$(2.5 \pm 1.8) \times 10^{-5}$	$(0.9 \pm 1.1) \times 10^{-5}$
2-heptanone	$(2.9 \pm 1.9) \times 10^{-6}$	$(9.5 \pm 7.6) \times 10^{-6}$	$(3.9 \pm 2.2) \times 10^{-6}$
6-methyl-2-heptanone	$(3.3 \pm 1.6) \times 10^{-5}$	$(2.5 \pm 1.8) \times 10^{-5}$	$(1.3 \pm 0.6) \times 10^{-7}$
2-methylfuran	$(2.9 \pm 0.8) \times 10^{-4}$	$(8.0 \pm 3.4) \times 10^{-5}$	$(2.0 \pm 3.3) \times 10^{-5}$
3-methylfuran	$(5.0 \pm 1.0) \times 10^{-5}$	$(1.8 \pm 0.2) \times 10^{-5}$	$(5.2 \pm 8.0) \times 10^{-6}$
Tetrahydrofuran	$(2.5 \pm 0.6) \times 10^{-5}$	$(2.4 \pm 1.7) \times 10^{-5}$	$(0.9 \pm 1.1) \times 10^{-5}$
2,3-dihydrofuran	$(2.1 \pm 0.7) \times 10^{-5}$	$(1.9 \pm 1.1) \times 10^{-5}$	$(0.8 \pm 1.0) \times 10^{-5}$
2-ethylfuran	$(6.0 \pm 3.5) \times 10^{-6}$	$(2.1 \pm 2.5) \times 10^{-6}$	$(0.9 \pm 1.3) \times 10^{-6}$
2,4-dimethyalfuran	$(4.1 \pm 1.1) \times 10^{-5}$	$(1.4 \pm 0.3) \times 10^{-5}$	$(4.2 \pm 6.5) \times 10^{-6}$
Benzofuran	$(2.9 \pm 1.2) \times 10^{-5}$	$(2.5 \pm 1.5) \times 10^{-5}$	$(7.8 \pm 9.2) \times 10^{-6}$
1-ethyl-2-methylbenzene	$(5.2 \pm 2.5) \times 10^{-6}$	$(3.8 \pm 2.9) \times 10^{-6}$	$(1.3 \pm 1.2) \times 10^{-6}$
1,2,4-trimethylbenzene	$(3.2 \pm 2.7) \times 10^{-6}$	$(0.9 \pm 1.3) \times 10^{-6}$	$(1.3 \pm 1.5) \times 10^{-6}$
1-ethyl-3-methylbenzene	$(7.8 \pm 1.1) \times 10^{-6}$	$(4.9 \pm 2.0) \times 10^{-6}$	$(2.6 \pm 3.7) \times 10^{-7}$
Propylbenzene	$(3.2 \pm 2.7) \times 10^{-6}$	$(2.1 \pm 2.1) \times 10^{-6}$	$(7.0 \pm 6.7) \times 10^{-7}$
o-xylene	$(2.9 \pm 0.8) \times 10^{-5}$	$(1.7 \pm 1.0) \times 10^{-5}$	$(6.8 \pm 9.4) \times 10^{-6}$
Ethylbenzene	$(2.8 \pm 1.1) \times 10^{-5}$	$(1.8 \pm 1.0) \times 10^{-5}$	$(6.6 \pm 1.1) \times 10^{-5}$
Toluene	$(4.6 \pm 2.3) \times 10^{-4}$	$(2.2 \pm 0.6) \times 10^{-4}$	$(5.7 \pm 8.7) \times 10^{-5}$
Benzene	$(8.8 \pm 1.3) \times 10^{-4}$	$(4.9 \pm 0.7) \times 10^{-4}$	$(3.1 \pm 1.8) \times 10^{-4}$
Phenol	$(1.0 \pm 0.6) \times 10^{-5}$	$(5.2 \pm 2.4) \times 10^{-6}$	$(1.8 \pm 2.8) \times 10^{-6}$

KNP, Kruger National Park.

the light hydrocarbons up to C_4 (figures in parentheses) and then all VOC. Taking into account the measured VOC the ozone mixing ratio increases steeper and earlier, because the ozone formation is now driven by the degradation of the hydrocarbons that react faster with OH than CO and CH_4. Ozone mixing ratios increase rapidly to values around 90 ppb within the first 2 hours after the emissions, followed by a further slower increase to about (175 ppb) 195 ppb. Thus the mixing ratio of ozone in the plume is about (30%) 45% larger if the impact of VOC is included with the peak mixing ratio reached about 30 hours after the emission. The initial NO_2 mixing ratio of 30 ppb was taken from the average of the measured data, which varied between 6 ppb and 60 ppb for different plume passages. The amount of ozone produced depends strongly on the NO_2 mixing ratio (Figure 5). Clearly, better temporally and spatially resolved NO_x data are necessary to further assess the impact of biomass burning to the global ozone budget.

To assess the total amount of ozone being produced, we have also calculated the excess ozone averaged over the final volume $V(t_e)$ denoted by $\langle \Delta O_3 \rangle$. The maximum $\langle \Delta O_3 \rangle$ was 150 ppb with VOC and 85 ppb without VOC.

The temporal behavior of the ozone mixing ratio in the plume of the sugar cane fire is similar to that of the Drakensberg fire, although the sugar cane combustion is different from that at Drakensberg. For the sugar cane fire the dilution factor was $D = 13$ and the time constant was again $\tau = 2$ hours. The most striking difference is the much larger initial NO_2 burden of 200 ppb inferred from the average of the measured data. The larger initial NO_2 and CO mixing ratios compared with the Drakensberg case causes the substantially smaller difference between the cases with and without VOC. The maximum $\langle \Delta O_3 \rangle$ for the sugar cane fire plume was 68 ppb including all measured VOC and 62 ppb without VOC. The results of this simple simulation show that in these cases, about 10 to 50% of the ozone formed in the plumes is due to the impact of VOC.

Global VOC Emissions

The analysis of NOAA AVHRR data indicates that in 1992 the burning season in southern Africa occurred between July

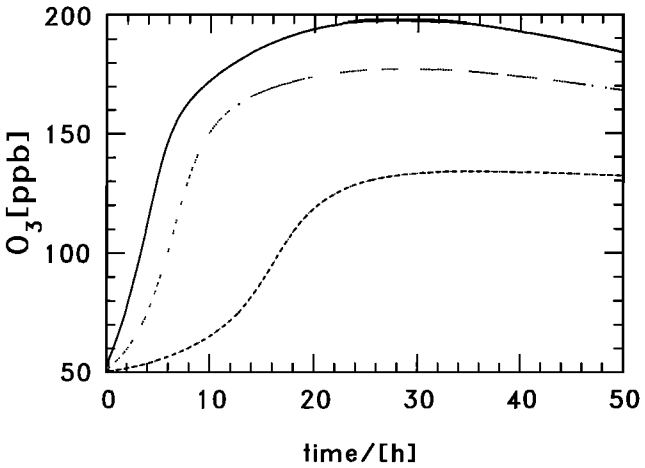

Figure 4. Model results for the time dependence of the ozone mixing ratio. The initial mixing ratios were taken from the Drakensberg fire. The dashed line shows results for the calculation without VOC, the dotted line shows the calculation with light NMHC up to C_4, and the solid line shows the calculation with all measured VOC.

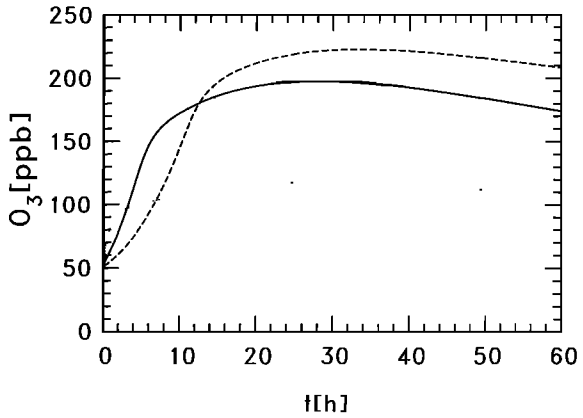

Figure 5. Model results for the time dependence of the ozone mixing ratio. The initial mixing ratios were taken from the Drakensberg fire. The curves refer to different initial NO_2 mixing ratios. The dashed line shows initial NO_2 = 60 ppb, the solid line shows initial NO_2 = 30 ppb, and the dotted line shows initial NO_2 = 6 ppb.

and September with the SAFARI campaign covering the end of the burning season. Furthermore, in 1992 there was about 50% less burning than in 1989 [*Justice et al.*, 1996]. It should be added that the samples are not likely to be representative for biomass burning on a global scale, since they represent only a very limited fraction of the areas burned globally each year. Therefore any extrapolations of our emission ratios to global scales are highly uncertain. In order to get an idea about the impact of biomass burning emissions to atmospheric chemistry, it is nevertheless worthwhile to compare the emissions of organic trace gases with global budgets. Table 5 summarizes the emission of total carbon species and CO from the various types of biomass burning based on a compilation of literature data [*Andreae*, 1991, 1993; *Hao and Liu*, 1994; *Andreae et al.*, 1996; and references therein]. Since the emissions of VOC are better correlated with CO than with CO_2, we base our extrapolation on VOC/CO emission ratios. If we use the emission ratios from the sugar cane fire 2 as a lower limit (mean $\Delta(VOC)/\Delta(CO)$ = 0.08%) and those from the Drakensberg fire as an upper limit (mean $\Delta(VOC)/\Delta(CO)$ = 0.15%), the estimated total carbon released in the form of VOC (CH_4 not included) ranges between 25 $\times$ 10^{12} g C/yr and 48 $\times$ 10^{12} g C/yr.

The higher molecular VOC contribute up to 50% to that value. This coarse estimate of the source strength of organic compounds based on our measurements is a factor of 2 higher than the results of previous estimates by *Bonsang et al.* [1991], who give 12 $\times$ 10^{12} g/yr derived from measurements over large savanna fires during the Dynamique et Chimie de l'Atmosphère en Forêt Equatoriale (DECAFE) project in the Ivory Coast. This number is below the lower limit of the emission range based on our estimates because *Bonsang et al.* [1991] based their estimates on measurements of light NMHC only. From laboratory studies, *Lobert et al.* [1991] calculate 42 $\times$ 10^{12} g/yr, a value at the upper end of our estimation range. These results indicate that the emissions from biomass burning contribute significantly to the local and regional budget of organic compounds in the troposphere.

Summary and Conclusions

In all samples collected in the plumes of the savanna and agricultural fires during SAFARI, a large variety of organic trace gases was found. They include alcohols, aldehydes, ketones, carboxylic acids, esters, ethers, furanes, and others. The observed emission ratios show a considerable variation depending on the fuel type and the burning conditions and stages of the fires. The emission ratio of the sum of light VOC was in the same order of magnitude as or even higher than that of methane. Our results show that higher-molecular-weight and oxygenated compounds, most of which are highly reactive, contribute significantly to the load of volatile organic compounds in biomass-burning emissions. Presently, roughly 70 of

Table 5. Emissions of Total Carbon Species and CO From the Various Types of Biomass Burning

Source	Biomass Burned (Dry Matter), Tg/yr	Carbon Released, Tg/yr	CO Emission Ratio, %	CO Emission, Tg C/yr
Tropical forest	1260	567	10.9	62
Extratropical forest	1150	518	11.2	58
Savanna	3690	1661	6.2	103
Biomass fuel	1940	873	8.3	73
Charcoal	21	42	20.0	8
Agricultural waste in fields	850	383	7.2	28
Total	8911	4043	8.2	331

some 140 major compounds could be identified in the samples, a number of which were previously not known to be emitted by biomass burning and thus were not included in estimates of the influence on the regional atmospheric chemistry. The uncontrolled fire in the Drakensberg forest showed emission ratios of the sum of organic compounds relative to CO_2 of $(13.7 \pm 0.9) \times 10^{-3}$ (ppb C/ppb CO_2) which are the highest values found during this campaign.

Simple model calculations were carried out in order to investigate the temporal development of the chemical ozone formation and the contribution of the individual ozone precursors. The simulation for the Drakensberg fire shows a maximum excess ozone with and without taking into account the impact of VOC of 150 ppb and 85 ppb, respectively, leading to 65 ppb of additional ozone in the plume due to the impact of VOC. For the sugar cane fire the simulation yields a maximum excess ozone of 68 ppb with VOC and 62 ppb without VOC, leading to 6 ppb of additional ozone due to the impact of VOC. Thus in the first case the impact of VOC is responsible for about 40% of additional ozone formed in the plumes, and in the second case it is responsible for <10%.

Our results show that higher-molecular-weight organic trace gases are a significant part of these emissions and play an important role for the photochemistry in biomass burning plumes. Their impact on the formation of tropospheric ozone is significant, especially during the initial phase of photochemical processing of biomass-burning emissions.

Acknowledgments. We thank the pilots and crews of the SAFARI-92 DC-3 research aircraft for their assistance during the research flights, the Kruger Park team (particularly A. Potgieter, W. Trollope, L. Trollope, and J. G. Goldammer) for their cooperation during the experimental fires in the park, and the team at the sugar plantation at Ubombo Ranches, Big Bend, Swaziland, (especially J. Gosnell and D. Shipley) for their generous help during our experiment. We acknowledge the permission of various government agencies in Angola, Botswana, South Africa, Namibia, Swaziland, Zambia, and Zimbabwe for permission to conduct research in these countries or to use the airspace over these countries. We appreciate the help of T. W. Andreae (logistical support) and U. Parchatka (technical support) during the airborne sampling missions on the DC-3 aircraft. Partial support of DC-3 aircraft program by the National Science Foundation is gratefully acknowledged. This research was part of IGBP/IGAC and was supported by the Max Planck Society and the Federal Ministry for Education, Research, and Technology (BMBF) under grant 105252 A 2b-6.

References

Albini, F. A., Dynamics and modeling of vegetation fires: Observations, in *Fire in the Environment: The Ecological, Atmospheric, and Climatic Importance of Vegetation Fires*, edited by P. J. Crutzen and J. G. Goldammer, pp. 39–52, John Wiley, New York, 1993.

Andreae, M. O., Biomass burning: Its history, use, and distribution and its impact on environmental quality and global climate, in *Global Biomass Burning: Atmospheric, Climatic, and Biospheric Implications*, edited by J. S. Levine, pp. 3–21, MIT Press, Cambridge, Mass., 1991.

Andreae, M. O., The influence of tropical biomass burning on climate and the atmospheric environment, in *Biogeochemistry of Global Change: Radiatively Active Trace Gases*, edited by R. S. Oremland, pp. 113–150, Chapman and Hall, New York, 1993.

Andreae, M. O., et al., Biomass burning in the global environment: First results from the IGAC/BIBEX field campaign STARE/TRACE-A/SAFARI-92, in *Global Atmospheric-Biospheric Chemistry, Environ. Sci. Res.*, vol. 48, edited by R. G. Prinn, pp. 83–101, New York, 1994.

Andreae, M. O., E. Atlas, H. Cachier, W. R. Cofer III, G. W. Harris, G. Helas, R. Koppmann, J. P. Lacaux, and D. E. Ward, Trace gas and aerosol emissions from savanna fires, in *Biomass Burning and Global Change*, edited by J. S. Levine, pp. 278–295, MIT Press, Cambridge, Mass., 1996.

Bonsang, B., G. Lambert, and C. Boissard, Light hydrocarbon emissions from African savanna burnings, in *Global Biomass Burning: Atmospheric, Climatic, and Biospheric Implications*, edited by J. S. Levine, pp. 155–166, MIT Press, Cambridge, Mass., 1991.

Chatfield, R. B., and A. C. Delany, Convection links biomass burning to increased tropical ozone; however, models will tend to overpredict O_3, *J. Geophys. Res.*, *95*, 18,473–18,488, 1990.

Crutzen, P. J., A. C. Delany, J. Greenberg, P. Haagenson, L. Heidt, R. Lueb, W. Pollock, W. Seiler, A. F. Wartburg, and P. Zimmerman, Tropospheric chemical composition measurements in Brazil during the dry season, *J. Atmos. Chem.*, *2*, 233–256, 1985.

Czapiewski, K., Emissionen von organischen Spurengasen aus Hausbrand im tropischen und subtropischen Afrika, diploma thesis, Carl-von-Ossietzky Univ., Oldenburg, Germany, 1995.

Delmas, R., On the emission of carbon, nitrogen, and sulfur in the atmosphere during bush fires in intertropical savanna zones, *Geophys. Res. Lett.*, *9*, 761–764, 1982.

Fishman, J., C. E. Watson, J. L. Larson, and J. A. Logan, Distribution of tropospheric ozone determined from satellite data, *J. Geophys. Res.*, *95*, 3599–3617, 1990.

Fishman, J., M. Hoell, Jr., R. D. Bendura, R. J. McNeal, and V. W. J. H. Kirchhoff, The NASA GTE TRACE-A Experiment (September–October 1992), *J. Geophys. Res.*, *101*, 23,865–23,879, 1996.

Franke, W., *Nutzpflanzenkunde*, Thieme-Verlag, Stuttgart, Germany, 1989.

Greenberg, J. P., and P. R. Zimmerman, Nonmethane hydrocarbons in remote tropical, continental, and marine atmospheres, *J. Geophys. Res.*, *89*, 4767–4778, 1984.

Greenberg, J. P., P. R. Zimmerman, L. Heidt, and W. Pollock, Hydrocarbon and carbon monoxide emissions from biomass burning in Brazil, *J. Geophys. Res.*, *89*, 1350–1354, 1984.

Greenberg, J. P., P. R. Zimmerman, W. F. Pollock, R. A. Lueb, and L. E. Heidt, Diurnal variability of atmospheric methane, nonmethane hydrocarbons, and carbon monoxide at Mauna Loa, *J. Geophys. Res.*, *97*, 10,395–10,413, 1992.

Hao, W. M., and M.-H. Liu, Spatial and temporal distribution of tropical biomass burning, *Global Biogeochem. Cycles*, *8*, 495–503, 1994.

Heidt, L., Whole air collection and analysis, *Atmos. Technol.*, *9*, 3–7, 1978.

Helas, G., et al., Ozone production due to emissions from vegetation burning, *J. Atmos. Chem.*, *22*, 163–174, 1995.

Hurst, D. F., D. W. T. Griffith, J. N. Carras, D. J. Williams, and P. J. Fraser, Measurements of trace gases emitted by Australian savanna fires during the 1990 dry season, *J. Atmos. Chem.*, *18*, 33–56, 1994.

Justice, C. O., J. D. Kendall, P. R. Dowty, and R. J. Scholes, Satellite remote sensing of fires during the SAFARI campaign using NOAA advanced very high resolution radiometer data, *J. Geophys. Res.*, *101*, 23,851–23,863, 1996.

Koppmann, R., R. Bauer, F. J. Johnen, C. Plass, and J. Rudolph, The distribution of light nonmethane hydrocarbons over the Mid-Atlantic: Results of the *Polarstern* cruise ANT VII/1, *J. Atmos. Chem.*, *15*, 215–234, 1992.

Koppmann, R., F. J. Johnen, C. Plass-Dülmer, and J. Rudolph, Distribution of methylchloride, dichloromethane, trichloroethene and tetrachloroethene over the North and South Atlantic, *J. Geophys. Res.*, *98*, 20,517–20,526, 1993.

Koppmann, R., F. J. Johnen, A. Khedim, J. Rudolph, A. Wedel, and B. Wiards, The influence of ozone on light nonmethane hydrocarbons during cryogenic preconcentration, *J. Geophys. Res.*, *100*, 11,383–11,391, 1995.

Lacaux, J. P., J. M. Brustet, R. Delmas, J. C. Menaut, L. Abbadie, B. Bonsang, H. Cachier, J. Baudet, M. O. Andreae, and G. Helas, DECAFE 91: Biomass burning in the tropical savannas of Ivory Coast, An overview of the field experiment Fire of Savannas (FOS/DECAFE '91), *J. Atmos. Chem.*, *22*, 195–216, 1995.

Le Canut, P., M. O. Andreae, G. W. Harris, F. G. Wienhold, and T. Zenker, Airborne studies of emissions from savanna fires in southern Africa, 1, Aerosol emissions measured with a laser-optical particle counter, *J. Geophys. Res.*, *101*, 23,615–23,630, 1996.

Lelieveld, J., P. J. Crutzen, D. Jacob, and A. Thompson, Modeling of biomass burning influences on tropospheric ozone, in *Fire in South African Savanna: Ecological and Atmospheric Perspectives*, edited by J. A. Lindesay, M. O. Andreae, P. D. Tyson, and B. van Wilgen, pp.

217–238, Univ. of Witwatersrand Press, Johannesburg, South Africa, 1997.

Levine, J. S., Global biomass burning: Atmospheric, climatic, and biospheric implications, in *Global Biomass Burning: Atmospheric, Climatic, and Biospheric Implications*, edited by J. S. Levine, pp. XXV–XXX, MIT Press, Cambridge, Mass., 1991.

Lobert, J. M., and J. Warnatz, Emissions from the combustion process in vegetation, in *Fire in the Environment: The Ecological, Atmospheric, and Climatic Importance of Vegetation Fires*, edited by P. J. Crutzen and P. J. Goldammer, pp. 15–37, John Wiley, New York, 1993.

Lobert, J. M., D. H. Scharffe, W. M. Hao, T. A. Kuhlbusch, R. Seuwen, P. Warneck, and P. J. Crutzen, Experimental evaluation of biomass burning emissions: Nitrogen and carbon containing compounds, in *Global Biomass Burning: Atmospheric, Climatic, and Biospheric Implications*, edited by J. S. Levine, pp. 289–304, MIT Press, Cambridge, Mass., 1991.

Manø, S., Messung von partiell oxidierten Kohlenwasserstoffen in Emissionen von Biomasseverbrennung, Ph.D. thesis, Johann-Wolfgang-von-Goethe-Univ., Frankfurt, Germany, 1997.

Rasmussen, P. R., and M. A. Khalil, Isoprene over the Amazon basin, *J. Geophys. Res.*, *93*, 1417–1421, 1988.

Rudolph, J., F. J. Johnen, and A. Khedim, Problems connected with the analysis of hydrocarbons and halocarbons in the non-urban atmosphere, *Int. J. Environ. Anal. Chem.*, *27*, 97–122, 1986.

Rudolph, J., K. P. Müller, and R. Koppmann, Sampling of organic volatiles in the atmosphere at moderate and low pollution levels, *Anal. Chim. Acta*, *236*, 197–211, 1990.

Rudolph, J., A. Khedim, and B. Bonsang, Light hydrocarbons in the tropical boundary layer over tropical Africa, *J. Geophys. Res.*, *97*, 6181–6186, 1992.

Rudolph, J., A. Khedim, R. Koppmann, and B. Bonsang, Field study of the emission of methyl chloride and other halocarbons from biomass burning in western Africa, *J. Atmos. Chem.*, *22*, 67–80, 1995.

Stocks, B. J., B. W. van Wilgen, W. S. W. Trollope, D. J. McRae, J. A. Mason, F. Weirich, and A. L. F. Potgieter, Fuels and fire behavior on large-scale savanna fires in Kruger National Park, South Africa, *J. Geophys. Res.*, *101*, 23,541–23,550, 1996.

Stockwell, W. R., P. Middleton, J. S. Chang, and X. Tang, The second generation regional acid deposition model chemical mechanism for regional air quality modeling, *J. Geophys. Res.*, *95*, 16,343–16,367, 1990.

Swap, R., M. Garstang, S. A. Macko, P. D. Tyson, W. Maenhaut, P. Artaxo, P. Kållberg, and R. Talbot, The long-range transport of southern African aerosols to the tropical South Atlantic, *J. Geophys. Res.*, *101*, 23,777–23,791, 1996.

Thompson, A. M., K. E. Pickering, D. P. McNamara, M. R. Schoeberl, R. D. Hudson, J. H. Kim, E. V. Browell, J. Fishman, V. W. J. H. Kirchhoff, and D. Nganga, Where did tropospheric ozone over southern Africa and the tropical Atlantic come from in October 1992?, Insights from TOMS, GTE TRACE-A and SAFARI 92, *J. Geophys. Res.*, *101*, 24,251–24,278, 1996.

Zimmerman, P. R., J. P. Greenberg, and C. E. Westberg, Measurements of atmospheric hydrocarbons and biogenic emission fluxes in the Amazon boundary layer, *J. Geophys. Res.*, *93*, 1407–1416, 1988.

M. O. Andreae, G. Helas, M. Welling, and T. Zenker, Max-Planck-Institut für Chemie, Postfach 3060, D-55020 Mainz, Federal Republic of Germany.

A. Khedim, R. Koppmann, D. Poppe, and J. Rudolph, Institut für Atmosphärische Chemie, ICG-3, Forschungszentrum Jülich, D-52425 Jülich, Federal Republic of Germany. (e-mail: r.koppmann@kfa-juelich.de)

(Received June 25, 1996; revised February 21, 1997;
accepted March 14, 1997.)